Theoretical and Experimental Analysis of a 4 × 4 Reconfigurable MZI-Based Linear Optical Processor

Farhad Shokraneh, Mohammadreza Sanadgol Nezami, and Odile Liboiron-Ladouceur, *Senior Member, IEEE*

***Abstract*—A 4 × 4 reconfigurable Mach–Zehnder interferometer (MZI)-based linear optical processor is investigated through its theoretical analyses and characterized experimentally. The linear transformation matrix of the structure is theoretically determined using its building block, which is a 2 × 2 reconfigurable MZI. To program the device, the linear transformation matrix of a given application is decomposed into that of the constituent MZIs of the structure. Thus, the required phase shifts for implementing the transformation matrix of the application by means of the optical processor are determined theoretically. Due to random phase offsets in the MZIs resulting from fabrication process variations, they are initially configured through an experimental protocol. The presented calibration scheme allows to straightforwardly characterize the MZIs to mitigate the possible input phase errors and determine the bar and cross states of each MZI for tuning it at the required sate before programming the device. After the configuration process, the device can be programmed to construct the linear transformation matrix of the application. In this regard, using the required bias voltages, the phase shifts obtained from the decomposition process are applied to the phase shifters of the MZIs in the device.**

***Index Terms*—Optical neural networks, optical matrix multiplication structures, reconfigurable linear optical processors.**

I. Introduction

THE interest in reconfigurable multiport linear optical interferometers is growing rapidly, due to their high speed and low power consumption. The interesting property of such structures is that they can be experimentally configured through theoretical analyses. In this regard, the phase shifters in such a mesh of MZIs are employed for its simple experimental calibration, which makes the structure suitable candidate to serve as a reconfigurable linear optical processor [1]–[3]. This paper presents the theoretical and experimental analysis of a 4 × 4 reconfigurable MZI-based optical processor that can be configured for a given application to perform linear functions, such as matrix multiplications in computational systems like optical neural networks [3], [4] quantum transport simulations [5], reconfigurable true-time optical delay lines [1] and singular value decomposition (SVD) in optics [6], [7]. They have also been used in different integrated optical structures representing linear transformation between inputs and outputs [2], [8], [9]. We start with a special unitary group of degree two i.e., SU(2), which is implemented by a 2 × 2 MZI tuned with one thermo-optic phase-shifter in one of its internal arms and another one at one of its output arms. The unitary transformation matrix of the reconfigurable MZI is determined by the product of the transformation matrices of its directional couplers and phase-shifters. Similarly, the linear transformation matrix of a reconfigurable multi-port optical processor can be obtained by the product of the unitary transformation matrices of its constituent MZIs. The main section of the 4 × 4 structure is an SU(4) of which linear transformation matrix can be calculated by the successive multiplications of that of its MZIs. The programming process of the SU(4) for a given application is equivalent to the decomposition of its linear transformation matrix into that of its constituent MZIs. We show how the decomposition process of a linear transformation matrix is used to determine the required phase shifts to implement it in optics. Our experimental characterization results show that the MZIs in the device exhibit random phase offsets originating from fabrication process variations. Thus, all the MZIs in the device are characterized experimentally through a presented calibration scheme prior to programming it for a given application. Finally, an arbitrary transformation matrix as an example is decomposed into the unitary transformation matrices of the MZIs in the 4 × 4 optical processor. We show how to determine the required phase shifts and their corresponding bias voltages to program the optical processor experimentally.

Manuscript received January 17, 2019; revised November 20, 2019; accepted January 10, 2020. Date of publication January 16, 2020; date of current version March 17, 2020. *(Corresponding author: Farhad Shokraneh.)*

The authors are with the Department of Electrical and Computer Engineering, McGill University, Montréal, Quebec, H3A 0E9, Canada (e-mail: farhad.shokraneh@mail.mcgill.ca; mohammadreza.sanadgolnezami@mail.mcgill.ca; odile@ieee.org).

Color versions of one or more of the figures in this article are available online at https://ieeexplore.ieee.org.

Digital Object Identifier 10.1109/JLT.2020.2966949

II. Theory and Analysis

A. 2 × 2 Reconfigurable MZI

A reconfigurable MZI-based linear optical processor is a compact and energy-efficient integrated device that can perform matrix multiplications with a low power consumption and at high speed, thanks to the inherent parallelism in optics [9], which leads to a linear computational time complexity as compared to the conventional processors with higher order ones [10]. Fig. 1 shows the schematic of a 2 × 2 reconfigurable MZI, which is the building block of a reconfigurable MZI-based linear optical processor.

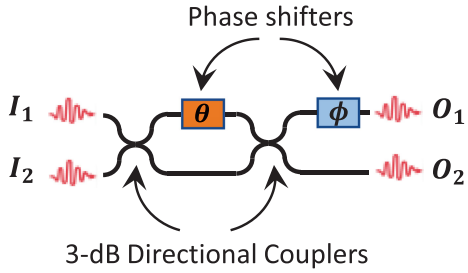

Fig. 1. Schematic illustration of the 2×2 reconfigurable MZI as the building-block of a multiport reconfigurable MZI-based linear optical processor.

The 2×2 reconfigurable MZI consists of two 3-dB (50:50) directional couplers with one phase shifter (θ) on one of the internal arms of the MZI and an external phase shifter (ϕ) at one of the outputs after the second directional coupler of the MZI. The internal phase shifter controls the power at the MZI outputs. The external one determines the relative phase of the MZI outputs, which allows for any rotation in special unitary group of degree two, i.e., SU(2). Thus, it can be configured by adjusting its two phase shifters by applying the required DC voltages. The linear transformation matrix of the reconfigurable MZI for a fixed state of polarization and lossless propagation can be determined by the product of the transformation matrices of its two 3-dB directional couplers with the power splitting ratio of $\rho = 0.5$ and the phase shifters of θ and ϕ as the following

$$
\begin{aligned}
[D_{MZI}] = \begin{pmatrix} u_{11} & u_{12} \\ u_{21} & u_{22} \end{pmatrix} &= \begin{pmatrix} e^{j\phi} & 0 \\ 0 & 1 \end{pmatrix} \cdot \begin{pmatrix} \sqrt{\rho} & j\sqrt{1-\rho} \\ j\sqrt{1-\rho} & \sqrt{\rho} \end{pmatrix} \\
&\cdot \begin{pmatrix} e^{j\theta} & 0 \\ 0 & 1 \end{pmatrix} \cdot \begin{pmatrix} \sqrt{\rho} & j\sqrt{1-\rho} \\ j\sqrt{1-\rho} & \sqrt{\rho} \end{pmatrix} \\
&= j e^{j\left(\frac{\theta}{2}\right)} \begin{pmatrix} e^{j\phi} \sin\left(\frac{\theta}{2}\right) & e^{j\phi} \cos\left(\frac{\theta}{2}\right) \\ \cos\left(\frac{\theta}{2}\right) & -\sin\left(\frac{\theta}{2}\right) \end{pmatrix}. \qquad (1)
\end{aligned}
$$

where u_{pq}, $(p, q \in \{1, 2\})$ represents the elements of the unitary transformation matrix of the reconfigurable MZI, which is also referred to as the linear optical Bogoliubov transformation matrix as it relates the inputs to the outputs linearly.

B. 4 × 4 Reconfigurable Linear Optical Processor

An $N \times N$ structure with n ($n = N(N-1)/2$) constituent MZIs can perform any rotation of a special unitary group of degree N (SU(N)), where N denotes the number of main channels from N input ports to N output ports, i.e., $I_s - O_s$ for $s = 1, 2, 3, N$. Each MZI can be reconfigured individually by controlling its two phase shifters. The phases of external phase-shifters in successive layers can be considered as a combined differential phase, which allows for any rotation of SU(N). To construct the transformation matrix of an SU(N), the unitary matrix of each MZI is presented on a two-dimensional subspace within N-dimensional Hilbert space ($H_{N\times N}$) leaving $(N-2)$-dimensional subspace unchanged [9]. Therefore, the unitary transformation matrix of the n MZIs within an SU(N) can be expressed as

$$
\begin{aligned}
&\left[D^{(n)}_{MZI(s,t)}\right]_{H_{N\times N}} \\
&= \begin{pmatrix}
1 & 0 & & \cdots & \cdots & & \cdots & 0 \\
0 & 1 & \ddots & \cdots & \cdots & & \cdots & 0 \\
\vdots & \ddots & \ddots & & & & \vdots & \vdots \\
0 & \cdots & & u_{11} & u_{12} & & \cdots & 0 \\
0 & \cdots & & u_{21} & u_{22} & & \cdots & 0 \\
\vdots & \vdots & & & & \ddots & \ddots & \vdots \\
0 & \cdots & & \cdots & \cdots & \ddots & 1 & 0 \\
0 & 0 & & \cdots & \cdots & & 0 & 1
\end{pmatrix}_{N\times N}. \qquad (2)
\end{aligned}
$$

In other words, D_{MZI} is defined in an N-dimensional Hilbert space and changes a two-dimensional subspace of it, which is along the diagonal elements of 1's while the unchanged off-diagonal elements are 0's, i.e., similar to an identity matrix of degree N (I_N). The transformation matrix of an SU(N) with N main channels can be determined by the multiplication of the transformation matrices of the MZIs each of which is connected to two adjacent channels, s and t i.e., $s = t - 1$, $t = 2, 3, \ldots, N$. As shown in Fig. 2, the SU(4) section of the 4×4 optical processor has four main channels, i.e., $I_s - O_s$: $I_1 - O_1$, $I_2 - O_2$, $I_3 - O_3$ and $I_4 - O_4$, representing channels one to four, respectively. For instance, MZI (3) is connected to channels one and two ($s = 1$ and $t = 2$).

As shown in Fig. 2, the 4×4 optical processor in this work is composed of an SU(4) section followed by a diagonal matrix multiplication section (DMM). Depending on the application of interest, the DMM section can be used to extend the 4×4 optical processor to a larger structure by cascading it with another SU(4), as in [6] to perform SVD optically, or in [3] for deep-learning matrix multiplications in neural networks applications. As shown in the figure, the first section contains MZIs (1) to (6) constructing the unitary transformation matrix $[T_{SU(4)}]$, while the latter consists of MZIs labelled as (7) to (10) composing a diagonal matrix multiplication (DMM) section representing a diagonal matrix $[\Sigma]$. Each MZI in the structure can be configured by controlling the power and the relative phase of its output ports through tuning its internal and external phase shifter, respectively.

To construct SU(4), the unitary matrices of the MZIs (1) to (6) are defined on a two-dimensional subspace within a four-dimensional Hilbert space. Therefore, the device constructs a transformation matrix $[D]_{4\times4}$ that linearly relates an input signal vector $[I]_{4\times1}$ to its output one $[O]_{4\times1}$. For a given application, the internal and external phase shifters of each MZI are adjusted by appropriate bias voltages to implement $[D]_{4\times4}$ reflecting the linear optical wave interactions in the physical device [6].

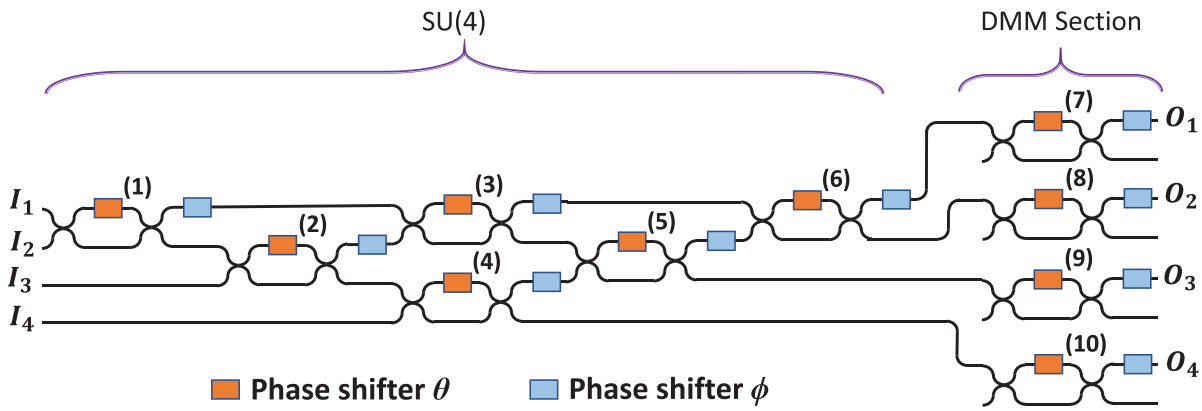

Fig. 2. Schematic illustration of the 4 × 4 MZI-based reconfigurable linear optical processor. The MZIs (1) to (6) implement SU(4), whereas the MZIs (7) to (10) construct the DMM section.

Thus, the linear transformation matrix of the structure can be determined by

$$[D]_{4\times4} = [\Sigma]\cdot[T_{SU(4)}] = \begin{pmatrix} u_{11}^{(7)} & 0 & 0 & 0 \\ 0 & u_{11}^{(8)} & 0 & 0 \\ 0 & 0 & u_{11}^{(9)} & 0 \\ 0 & 0 & 0 & u_{11}^{(10)} \end{pmatrix} \cdot \begin{pmatrix} U_{11} & U_{12} & U_{13} & U_{14} \\ U_{21} & U_{22} & U_{23} & U_{24} \\ U_{31} & U_{32} & U_{33} & U_{34} \\ U_{41} & U_{42} & U_{43} & U_{44} \end{pmatrix}, \tag{3}$$

where U_{kl} (k and $l \in \{1, 2, 3, 4\}$) are elements in $[T_{SU(4)}]$, which can be determined by the product of matrices $[D_{MZI}^{(n)}]$ with $u_{pq}^{(n)}$, for p, q $\in \{1, 2\}$ and $n \in \{1, 2, \ldots, 6\}$. $[T_{SU(4)}]$ represents the unitary transformation matrix of SU(4) and can be obtained by the product of the unitary transformation matrices of MZIs (1) to (6) depending upon their location in the structure, being connected to channels s and t, ($s = t - 1$, $t = 2, 3, 4$). For instance, MZI (1) is connected to channels one and two, $s = 1$, and $t = 2$. Therefore, the unitary transformation matrix is defined as the following

$$[T_{SU(4)}] = [D_{MZI}^{(6)}]_{H_{4\times4}} \cdot [D_{MZI}^{(5)}]_{H_{4\times4}} \cdot [D_{MZI}^{(4)}]_{H_{4\times4}} \cdot [D_{MZI}^{(3)}]_{H_{4\times4}} \cdot [D_{MZI}^{(2)}]_{H_{4\times4}} \cdot [D_{MZI}^{(1)}]_{H_{4\times4}}. \tag{4}$$

C. Programming the Linear Optical Processor

The programming process of an $N \times N$ reconfigurable MZI-based linear optical processor is carried out based on the decomposition of the linear transformation matrix of $[T_{SU(N)}]$ into the unitary matrices of the corresponding MZIs in the device. To this end, the unitary transformation matrix $[T_{SU(N)}]$ given by an application is successively multiplied by the $[D_{MZI}^{(n)}]_{H_{N\times N}}^{-1}$ from the right. In this regard, the inverse unitary transformation matrices of the MZIs are also represented on a two-dimensional subspace within an N-dimensional Hilbert space with an $(N - 2)$-dimensional unchanged subspace. Due to the unitary property of the transformation matrix of each reconfigurable MZI, its inverse $[D_{MZI}]^{-1}$ is equivalent to its conjugate transpose, which can be given by

$$[D_{MZI}]^{-1} = -je^{-j(\frac{\theta}{2})} \begin{pmatrix} e^{-j\phi}\sin\left(\frac{\theta}{2}\right) & \cos\left(\frac{\theta}{2}\right) \\ e^{-j\phi}\cos\left(\frac{\theta}{2}\right) & -\sin\left(\frac{\theta}{2}\right) \end{pmatrix}. \tag{5}$$

The decomposition process of $[T_{SU(N)}]$ is equivalent to a reverse experimental setup, i.e., the light is coupled to the device from the right side of the device, where the output ports are used as inputs to couple the light and the input ports are used as outputs to measure. As a result, the successive products should be done in an specific order starting from the left first layer of MZIs, which face the ports on the left side of the device. It is essential to note that in each step of the successive multiplications of $[T_{SU(N)}]$ by $[D_{MZI}^{(n)}]_{H_{4\times4}}^{-1}$, an off-diagonal element in the lower triangle of the resultant matrix becomes zero, a method similar to Gaussian elimination. Due to the unitary property of the resultant matrices in every step, once an off-diagonal element becomes zero, it will not be changed by the next transformations. Moreover, in each row, when all off-diagonal elements become zero, the off-diagonal elements in the corresponding column also become zero in accordance with the unitarity. Thus, after the successive multiplications in a row, the effective dimension of the resultant matrix is reduced by one [9]. Thus,

$$[T_{SU(N)}]\cdot[D_{MZI(N,1)}]_{H_{N\times N}}^{-1}\cdot[D_{MZI(N,2)}]_{H_{N\times N}}^{-1}\cdots [D_{MZI(N,N-1)}]_{H_{N\times N}}^{-1} = \begin{pmatrix} \begin{pmatrix} & T_{SU(N-1)} & \\ & & \\ & & \end{pmatrix} & \begin{matrix} 0 \\ \\ \end{matrix} \\ \begin{matrix} 0 & \end{matrix} & 1 \end{pmatrix}. \tag{6}$$

Eventually, this successive product results in an identity matrix $I_{(N\times N)}$. Consequently, the required phase shifts for programming the device can be determined with the limited number of multiplications in the decomposition process.

In the case of the 4 × 4 structure, during the programming process of the SU(4), MZIs (7) to (10) are tuned to be in their bar states. To decompose $[T_{SU(4)}]$, it is successively multiplied by the $[D_{MZI}^{(n)}]_{H_{4\times4}}^{-1}$ for $n = 1, 2, 3, \ldots, 6$ from the right. These

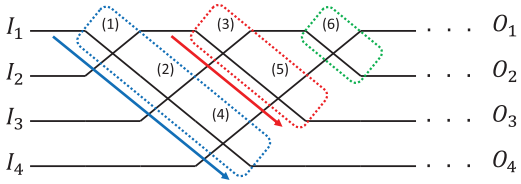

Fig. 3. Schematic illustration of the MZIs order in the SU(4) section for decomposing the unitary transformation matrix $[T_{SU(4)}]$ of a given application to program the 4×4 optical processor experimentally.

successive products are done in a specific order based on the equivalent reverse experimental setup. As can be seen in Fig. 3, the decomposition process starts from MZIs (1), (2), and (4) (blue box), and then MZIs (3) and (5) (red box) before MZI (6) (green box).

Therefore, the final resulting matrix is the identity matrix $I_{(4)}$.

$$[T_{SU(4)}] \cdot [D^{(1)}_{MZI}]^{-1}_{H_{4\times4}} \cdot [D^{(2)}_{MZI}]^{-1}_{H_{4\times4}} \cdot [D^{(4)}_{MZI}]^{-1}_{H_{4\times4}} \cdot [D^{(3)}_{MZI}]^{-1}_{H_{4\times4}} \cdot [D^{(5)}_{MZI}]^{-1}_{H_{4\times4}} \cdot [D^{(1)}_{MZI}]^{-1}_{H_{4\times4}} = I(4). \quad (7)$$

By making the off-diagonal elements zero, step by step, the required phase shifts in the inverse transformation matrix of the corresponding MZI ($[D^{(n)}_{MZI}]^{-1}_{H_{4\times4}}$) can be calculated. The steps for decomposing the linear transformation matrix of a given application can be expressed as

- *Step 1:* Considering the left first layer of MZIs (blue box) in Fig. 3, the product of $[T_{SU(4)}]$ with $[D^{(1)}_{MZI}]^{-1}_{H_{4\times4}}$ nulls the first element in the forth row of the resultant matrix,

$$[T_{SU(4)}] \cdot [D^{(1)}_{MZI}]^{-1}_{H_{4\times4}} = \begin{pmatrix} U_{11} & U_{12} & U_{13} & U_{14} \\ U_{21} & U_{22} & U_{23} & U_{24} \\ U_{31} & U_{32} & U_{33} & U_{34} \\ U_{41} & U_{42} & U_{43} & U_{44} \end{pmatrix}$$

$$\cdot -je^{-j(\frac{\theta_1}{2})} \begin{pmatrix} e^{-j\phi_1}\sin\left(\frac{\theta_1}{2}\right) & \cos\left(\frac{\theta_1}{2}\right) & 0 & 0 \\ e^{-j\phi_1}\cos\left(\frac{\theta_1}{2}\right) & -\sin\left(\frac{\theta_1}{2}\right) & 0 & 0 \\ 0 & 0 & 1 & 0 \\ 0 & 0 & 0 & 1 \end{pmatrix}$$

$$= \underbrace{\begin{pmatrix} * & * & * & * \\ * & * & * & * \\ * & * & * & * \\ 0 & * & * & * \end{pmatrix}}_{[\mathbf{A}]}, \quad (8)$$

where (*) denotes a matrix element, which is determined in a later step. Therefore, A_{41}, which is a function of phase θ_1 is set to zero and thus, θ_1 in MZI (1) can be calculated by

$$\theta_1 = 2 * \tan^{-1}\left(\frac{-U_{42}}{U_{41}}\right). \quad (9)$$

- *Step 2:* The product of [A] with $[D^{(2)}_{MZI}]^{-1}_{H_{4\times4}}$ nulls the second element on the fourth row of the resultant matrix [B] as follow

$$[A] \cdot [D^{(2)}_{MZI}]^{-1}_{H_{4\times4}} = \underbrace{\begin{pmatrix} * & * & * & * \\ * & * & * & * \\ * & * & * & * \\ 0 & 0 & * & * \end{pmatrix}}_{[\mathbf{B}]}. \quad (10)$$

Similarly, $B_{42}(\theta_2) = 0$ leads to the determination of the phase shift of θ_2 in MZI (2).

- *Step 3:* Likewise, the multiplication of [A] by $[D^{(4)}_{MZI}]^{-1}_{H_{4\times4}}$ sets the last off-diagonal elements in the last row of the resultant matrix [C] to zero, given by

$$[B] \cdot [D^{(4)}_{MZI}]^{-1}_{H_{4\times4}} = \underbrace{\begin{pmatrix} * & * & * & 0 \\ * & * & * & 0 \\ * & * & * & 0 \\ 0 & 0 & 0 & 1 \end{pmatrix}}_{[\mathbf{C}]}. \quad (11)$$

As a result, $C_{43}(\theta_4) = 0$ allows for obtaining the phase shift of θ_4 in MZI (4). It is essential to note that due to the unitary property of the resultant matrices, once all off-diagonal elements in a row become zero, the diagonal element is set to one and the off-diagonal elements in the corresponding column also become zero. Consequently, by determining θ_4 in MZI (4) in this step, $C_{44} = 1$ and $C_{14} = C_{24} = C_{34} = 0$, which means the effective dimension of the resultant matrix in this step is reduced by one as shown in equation (6).

- *Step 4:* The next step is to multiply [C] by $[D^{(3)}_{MZI}]^{-1}_{H_{4\times4}}$ corresponding to the red box in Fig. 3, which nulls the first element in the third row of the resultant matrix [D] given by

$$[C] \cdot [D^{(3)}_{MZI}]^{-1}_{H_{4\times4}} = \underbrace{\begin{pmatrix} * & * & * & 0 \\ * & * & * & 0 \\ 0 & * & * & 0 \\ 0 & 0 & 0 & 1 \end{pmatrix}}_{[\mathbf{D}]}, \quad (12)$$

$$D_{31}(\theta_3, \phi_1, \phi_2) = 0. \quad (13)$$

- *Step 5:* The product of [D] with $[D^{(5)}_{MZI}]^{-1}_{H_{4\times4}}$ sets the second element in the third row of the resultant matrix [E] expressed as

$$[D] \cdot [D^{(5)}_{MZI}]^{-1}_{H_{4\times4}} = \underbrace{\begin{pmatrix} * & * & 0 & 0 \\ * & * & 0 & 0 \\ 0 & 0 & 1 & 0 \\ 0 & 0 & 0 & 1 \end{pmatrix}}_{[\mathbf{E}]}, \quad (14)$$

$$E_{32}(\theta_3, \theta_5, \phi_1, \phi_2, \phi_4) = 0. \quad (15)$$

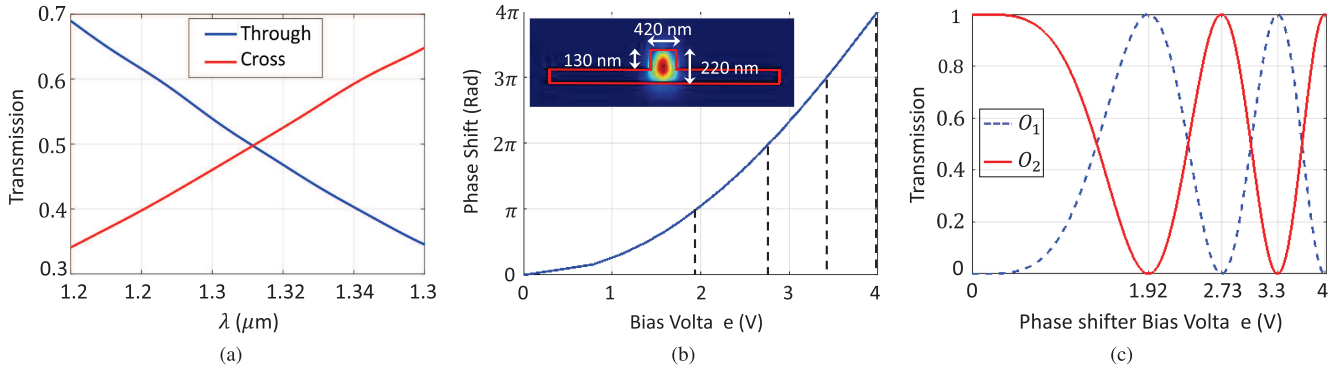

Fig. 4. Simulation results of the 3-dB directional coupler, the phase shifter, and the MZI designed for $\lambda = 1310$ nm: (a) transmission spectrum of the 3-dB directional coupler, (b) resultant phase shifts in the phase shifter for different bias voltages ([0–4] V), along with the electric field intensity of TE_0 mode in the ridge-waveguide with its dimensions, and (c) transmission of the MZI output ports as a function of the applied bias voltage to its internal phase shifter.

Since all the off-diagonal elements in the third row of the resultant matrix [E] are set to zero, it can be concluded that

$$E_{33}(\theta_3, \theta_5, \phi_1, \phi_2, \phi_4) = 1, \tag{16}$$

$$E_{23}(\theta_3, \theta_5, \phi_1, \phi_2, \phi_4) = 0, \tag{17}$$

$$E_{13}(\theta_3, \theta_5, \phi_1, \phi_2, \phi_4) = 0. \tag{18}$$

Using equations (13), (15), (16), (17), and (18), the phases shifts θ_3, θ_5, ϕ_1, ϕ_2 and ϕ_4 of the corresponding MZIs in the device can be determined.

- *Step 6:* The multiplication of [E] by $[D^{(6)}_{MZI}]^{-1}_{H_{4\times4}}$ nulls the first element of the second row in [F], expressed by

$$[E] \cdot [D^{(6)}_{MZI}]^{-1}_{H_{4\times4}} = \underbrace{\begin{pmatrix} 1 & 0 & 0 & 0 \\ 0 & 1 & 0 & 0 \\ 0 & 0 & 1 & 0 \\ 0 & 0 & 0 & 1 \end{pmatrix}}_{[\mathbf{F}]}, \tag{19}$$

$$F_{21}(\theta_6, \phi_3, \phi_5) = 0. \tag{20}$$

In this step, all the off-diagonal elements in the second row of [F] are set to zero, thus, similar to previous rows,

$$F_{22}(\theta_6, \phi_3, \phi_5) = 1, \tag{21}$$

$$F_{12}(\theta_6, \phi_3, \phi_5) = 0, \tag{22}$$

$$F_{11}(\theta_6, \phi_3, \phi_5, \phi_6) = 1. \tag{23}$$

In other words, [F] is the identity matrix, and using equations (20), (21), (22), and (23), the phases shifts θ_6, ϕ_3, ϕ_5 and ϕ_6 can be obtained. Therefore, all the required phase shifts to implement the linear transformation matrix by the 4×4 optical processor are determined. Using equation (4), these phase shifts can be applied to the MZIs in the optical processor to construct the linear transformation matrix of the given application, experimentally. An example for programming the optical processor for an arbitrary linear transformation matrix will be given in the following section.

III. Simulation and Experimental Results

A 2×2 reconfigurable MZI makes use of two phase shifters θ and ϕ to control the power and the relative phase of its outputs, respectively. As shown in Fig. 4, the devices and phase shifters in this paper are designed for 1310 nm of wavelength using a 220 nm $\times$ 420 nm cross-sectional-area ridge-based SOI waveguide with a 90-nm-hight slab, which were optimized through numerical analysis. Each phase shifter consists of five resistors each of which with 27 μm length [11]. Using Lumerical solvers, the 3-dB directional couplers are designed with an optimal length of 9.13 μm and a separation gap of 0.2 μm between the coupling waveguides [12], [13]. The physical dimensions of the ridge-based SOI waveguide, the directional coupler and the phase shifter can be designed for optimal performance at 1550 nm of wavelength as well. The incentives for choosing 1310 nm of wavelength are zero dispersion and low nonlinear effect for short reach applications [14]. According to the thermo-optic effect, the bias voltage heats the highly doped silicon slab of the phase shifter causing a temperature induced refractive index change in one of the arms of the MZI. Consequently, there is a phase shift in the light propagating in the waveguide of length L, due to the temperature-induced refractive index change at the wavelength of interest λ, given by θ or $\phi = \frac{2\pi L}{\lambda}(\frac{dn}{dT}) \triangle T$, where $\frac{dn}{dT} = 1.94 \times 10^{-4} K^{-1}$ is the thermo-optic coefficient of silicon at $\lambda = 1310$ nm.

Fig. 4 demonstrates the simulation results from Lumerical solutions of the designed 3-dB directional coupler, the phase shifter, and the reconfigurable MZI for TE_0 mode. According to the results shown in Fig. 4(b) and Fig. 4(c), the required bias voltages for switching power between the output ports of the MZI, corresponding to $\theta = \pi, 2\pi, 3\pi$ and 4π, are 1.92 V, 2.73 V, 3.38 V and 4 V, respectively.

Fig. 5 shows the microscope image of the fabricated 2×2 reconfigurable MZI. The designed devices in this paper were fabricated using 193 nm DUV lithography at the Institute of Microelectronics (A*STAR IME) through a multi-project wafer (MPW) service managed by Canadian Microelectronic Corporation (CMC). The fabricated 2×2 structure is tuned by applying proper bias voltages to its two phase shifters θ and ϕ. The two

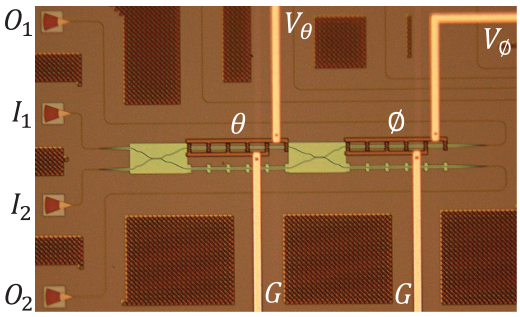

Fig. 5. Microscope image of the fabricated 2 × 2 reconfigurable MZI, which is the test structure of a multiport reconfigurable linear MZI-based processor.

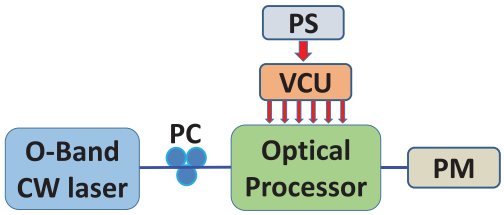

Fig. 6. Schematic block diagram of the experimental setup.

phase shifters are controlled by an off-chip voltage controlling unit (VCU) connected to their common ground pad G and the DC voltage pads, V_θ and V_ϕ, respectively.

Fig. 6 illustrates the schematic of the experimental setup of the single-mode transmission in this research work.

The continuous wave (CW) at 1310 nm is generated by a Keysight tunable O-band laser. The optical signal passes through a polarization controller (PC) to optimize the state of polarization to the TE_0 mode required by the device for single-mode polarization. The light is coupled to the input vertical grating coupler (GC) of the optical processor. A power supply (PS) is used to provide the electrical DC voltage for an off-chip voltage controlling unit (VCU) to tune the phase shifters of the MZIs with the required bias voltages. The output optical power is measure using an optical power meter (PM).

Fig. 7 depicts the measured I-V curve and the normalized optical power from the input ports I_1 and I_2 to the output ports O_1 and O_2 of the 2 × 2 reconfigurable MZI. The 2 × 2 structure is the test structure of the 4 × 4 reconfigurable linear optical processor in this work. As can be inferred from Fig. 7(a), the measured ohmic resistance of the phase shifter is approximately 170 Ω corresponding to approximately 21 mW switching power. According to Figs. 7(b) and 7(c), the worst-case switching extinction ratio (ER) is approximately 43 dB. The insertion loss (IL) of the single reconfigurable MZI is approximately −1.5 dB, which can be simply compensated by amplifying the input optical signal power using an optical amplifier. The required bias voltages for switching power between the outputs of the MZI are in good agreement with the simulation results shown in Fig. 4.

Fig. 8 demonstrates the microscope image of the 4 × 4 reconfigurable linear optical processor. The device can be reconfigured by applying the required DC bias voltages to the phase shifters of the MZIs through the corresponding electrical DC pads and the ground pads (G). The off-chip VCU is used to adjust the required DC voltages for the phase shifters. The structure can be developed to a larger multiport reconfigurable MZI-based processor using the MZIs (S1) and (S2). These two MZIs in the 4 × 4 structure are tuned to be in their bar states and work as simple waveguides.

Due to fabrication process variations affecting the phase shifters and the directional couplers, the MZIs in the structure are not ideal and thus, experiencing random phase offsets during measurements. Consequently, all the MZIs in the device need to be initially characterized for calibration purposes before programming the device for a given application. By characterizing the MZIs, their bar and cross states can be determined as reference states. Prior to programming the device, the MZIs are tuned in the required states, i.e., MZIs (1) to (6) should be in their cross states, while MZI (7) to (10), (S1), and (S2) are tuned in their bar states. As a result, the fabrication imperfections causing phase errors can be mitigated. The calibration process is carried out based on the structural topology of the device and the location of each MZI in the layouts of the device. Using the forward experimental setup where light is coupled from the inputs to the outputs of the device, each MZI is characterized on a path with the minimum number of uncharacterized MZIs. The optical power transmission of the MZI on the chosen path is measured as a function of the applied bias voltage to its internal phase shifter. This process determines the reference states of the MZI. As shown in Fig. 9, MZIs (4), (5) and (6) (blue box) on the paths from I_4 to O_1, O_2, O_3, and O_4, respectively, face the least number of unconfigured MZIs. Thus, they are simpler to access for calibration than other MZIs. The choice of these MZIs for configuration prior to other MZIs can also be associated with the fact presented by equations (11), (14) and (19) for the decomposition of $[T_{SU(4)}]$. According to these equations, the inverse transformation matrices of MZIs (4), (5) and (6) null the last off-diagonal element in each row of the lower triangle section, which also null the off-diagonal elements in the corresponding columns of the upper triangle part in the resultant matrices. This can be associated with their location in the structure and their simpler accessibility for configuration due to a smaller number of uncalibrated MZIs on the related path compared to the other layer of MZIs (red and green boxes). Similarly, the rest of the MZIs shown in Fig. 9 are characterized, respectively.

Fig. 10 summarizes the experimental configuration results of the MZIs in the 4 × 4 optical processor. To configure an MZI in the device, the normalized output optical power transmission of the MZI on the path with the minimum number of uncharacterized MZIs is measured as a function of the applied bias voltages [0–4] V to the phase shifter of the MZI. The calibration of MZI (4) on the path $I_4 - O_4$ and setting it in its C.S. allows for the characterization of MZI (5) on the path $I_4 - O_3$. Similarly, MZI (6) on the path $I_4 - O_2$ can be characterized while both MZI (4) and (5) are tuned in their C.S. MZIs (7), (8), (9) and (10) in the DMM section on the paths from I_4 to the corresponding output ports, are also characterized while the previously configured MZIs, i.e., the first layer of MZIs (blue box) in Fig. 9, are

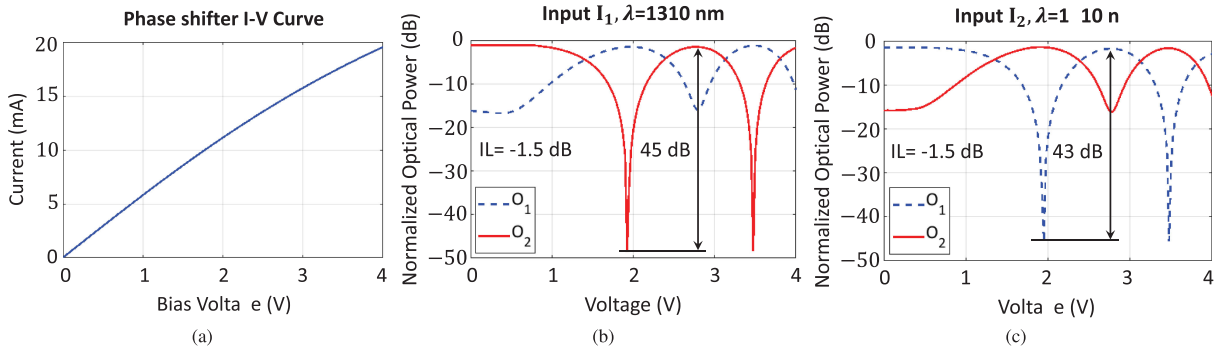

Fig. 7. Measurement results of the 2 × 2 reconfigurable MZI as a test structure; (a) measured I-V curve of the phase shifter, (b) and (c) normalized optical power of the 2 × 2 reconfigurable MZI from I_1 and I_2 input ports to O_1 and O_2 output ports as function of bias voltages.

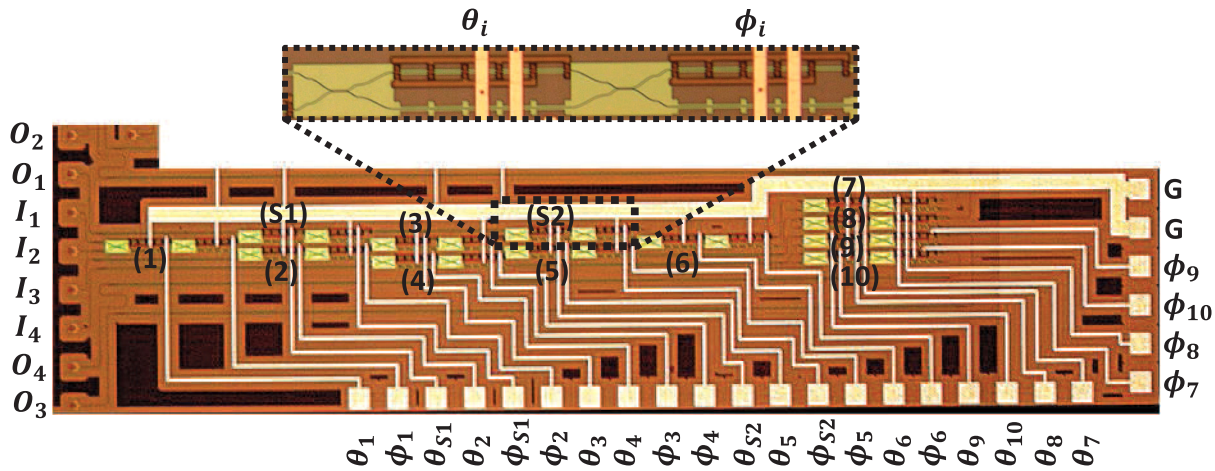

Fig. 8. Microscope image of the fabricated 4 × 4 MZI-based linear optical processor. Inset shows one of the reconfigurable MZIs in the structure. MZIs (1) to (6) implement $[T_{SU(4)}]$, whereas MZIs (7) to (10) construct $[\Sigma]$. The MZIs are tuned by the VCU, which is used to apply the required DC voltages to their phase shifters through the corresponding electrical DC voltage pads and two common ground pads (G) as shown in the figure. The MZIs (S1) and (S2) in an SU(4) are tuned to be in their bar states to serve as simple waveguides, however, they can be used to extend the device to a larger N-dimensional SU(N).

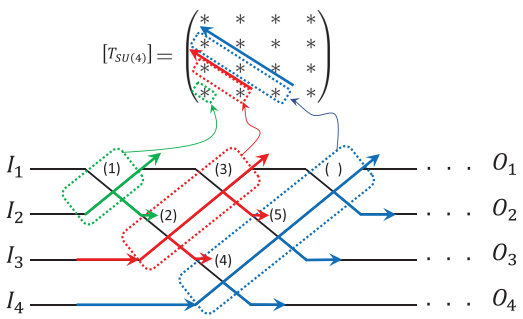

Fig. 9. Schematic of the characterization order of the MZIs in the SU(4).

configured in their proper states. MZIs (2) and (3) (red box) on the paths $I_3 - O_3$ and $I_3 - O_2$ can then be calibrated by tuning the earlier configured MZIs in the appropriate states. Finally, MZI (1) (green box) on the path $I_2 - O_2$ is characterized in a similar way. It is notable that MZIs (S2) and (S1) on the paths $I_3 - O_1$ and $I_2 - O_1$ are characterized while MZIs (1), (2), (3) and (7) are in the required states.

As shown in Fig. 10, the MZIs in the device exhibit random phase offsets originating from fabrication process variations in the waveguides, the phase shifters and the directional couplers. In terms of IL, different paths exhibit different IL values depending on the number of the MZIs on the paths and their switching states (B.S. or C.S. states). For instance, as shown in Fig. 10(a), MZI (4) on the path from I_4 to O_4, has its cross state (C.S.) at $V_{C.S.} \approx 2.25$ V and its bar state (B.S.) at $V_{B.S.} \approx 3.0$ V when MZI (10) has not been configured yet. By tuning MZI (4) in its B.S., the configuration of MZI (10) shows that when MZI (10) is in B.S., the IL of the path from I_4 to O_4 is approximately -3 dB, which is in good agreement with that of the single reconfigurable MZI measurements shown in Fig. 7, i.e., -1.5 dB per MZI. The higher IL values for some paths can be associated with the longer paths with a greater number of MZIs and also with fabrication process variations, e.g., $I_4 - O_1$ and $I_4 - O_2$.

Table I summarizes the experimental configuration results of the MZIs in the 4 × 4 optical processor, which presents the required DC voltages for their cross state (C.S.) and bar state (B.S.) configurations. Compared to the 2 × 2 test structure with $V_{C.S.} = 2.7$ V and $V_{B.S.} = 3.45$ V, the required $V_{C.S.}$ values of the MZIs in the 4 × 4 structure ranges from 2.25 V to 3.02 V, and $V_{B.S.}$ values vary from 3.0 V to 3.7 V. Depending on the required

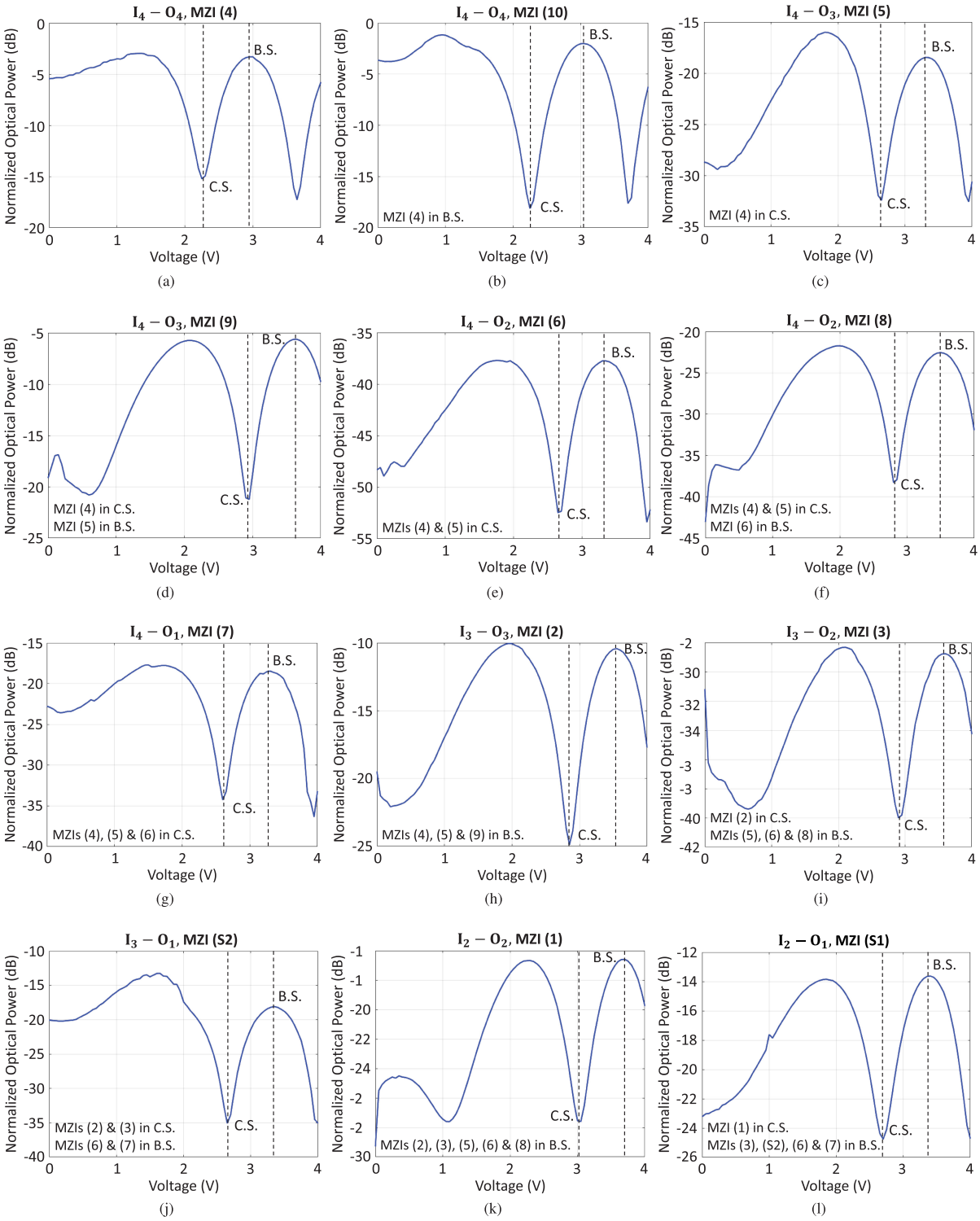

Fig. 10. Characterization process of the MZIs in the 4 × 4 structure for calibration purposes. Depending on the location of an MZI in the structure, the output optical power of the corresponding path is measured as a function of the applied voltages to its phase shifter. A configured MZI in previous steps is either in its bar state (B.S.) or cross state (C.S.) for characterization of an unconfigured MZI.

voltage to set an MZI in proper state, the thermal stabilization time for tuning every phase shifter in the device is observed to be less than 30 μs. The total electrical power consumption of the device for configuration of the MZIs in their appropriate states (MZI (1) to (10) in C.S., MZIs (S1) and (S2) in B.S.) is approximately 507 mW.

Fig. 11 shows the measurement results of the normalized optical power transmission spectra for the paths from I_4 to O_1, O_2, O_3 and O_4, as some examples, demonstrating the IL in each case and the corresponding crosstalk at the output ports. As can be inferred from Figs. 11(a), 11(b), 11(c) and 11(d), the IL values for $I_4 - O_4$, $I_4 - O_3$, $I_4 - O_2$ and $I_4 - O_1$ are

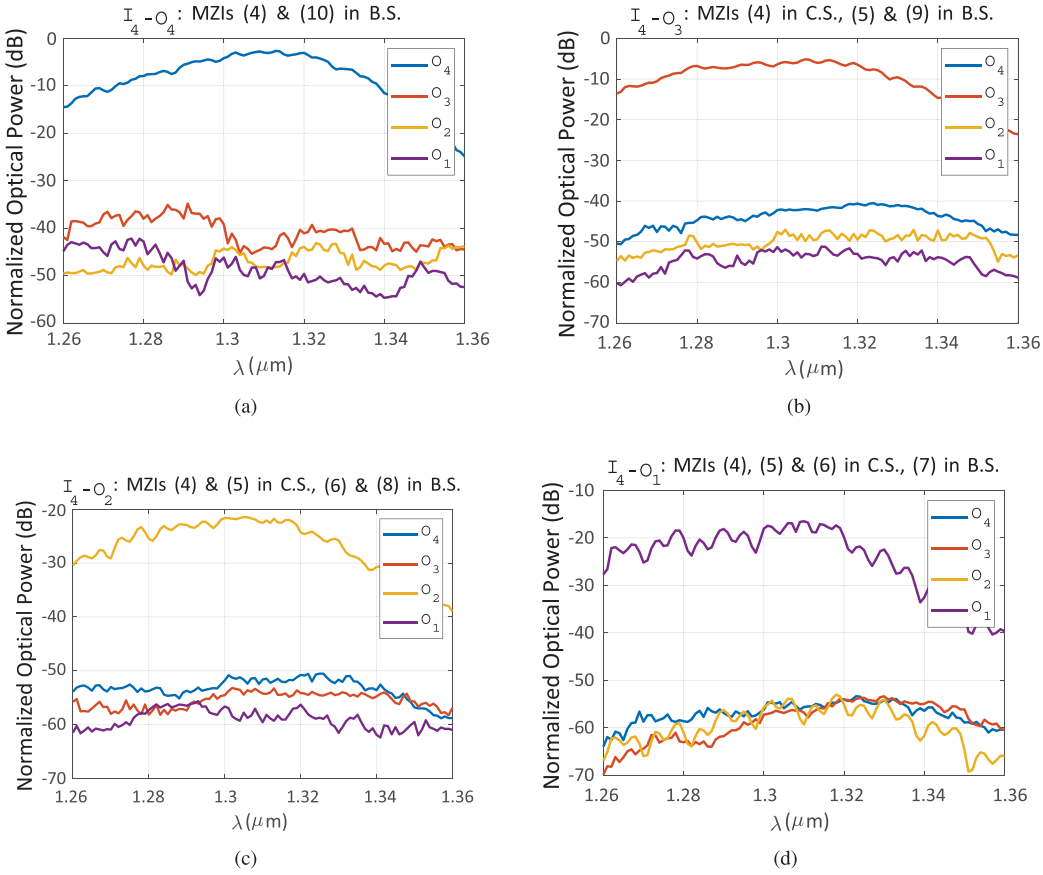

Fig. 11. Normalized optical power transmission spectra for $I_4 - O_4$, $I_4 - O_3$, $I_4 - O_2$ and $I_4 - O_1$ demonstrating the IL and crosstalk between the output ports in each scenario.

TABLE I
OBTAINED $V_{C.S.}$ AND $V_{B.S.}$ VALUES THROUGH THE EXPERIMENTAL CONFIGURATION OF THE MZIS IN THE 4 × 4 OPTICAL PROCESSOR

MZI	(1)	(2)	(3)	(4)	(5)	(6)
$V_{C.S.}$ (V)	3.02	2.85	2.92	2.25	2.64	2.67
$V_{B.S.}$ (V)	3.70	3.55	3.60	2.97	3.35	3.35
MZI	(7)	(8)	(9)	(10)	(S1)	(S2)
$V_{C.S.}$ (V)	2.60	2.82	2.93	2.25	2.65	2.70
$V_{B.S.}$ (V)	3.30	3.50	3.65	3.05	3.35	3.40

in good agreement with the experimental calibration results shown in Figs. 10(b), 10(d), 10(f) and 10(g) at the maximum normalized optical power levels of the corresponding output ports. According to the results in each case, the crosstalk values between the output ports are lower than −35 dB.

After characterizing the MZIs in the structures, the device is ready for being programmed by applying the required voltages to the phase shifters of the MZIs to construct the linear transformation matrix of a given application. To this end initially, the MZIs (1) to (6) are tuned to be in C.S. whereas the MZIs (S1), (S2) and MZIs (7) to (10) are set to be in B.S. This process is done by applying the required bias voltages to their phase shifters determined from the characterization process of the MZIs. The interesting property of the programmable optical processor is that the optical power at the output ports can be adjusted at any level of interest, by tuning the phase shifters of the MZIs appropriately. As shown in Figs. 2 and 8, there may be several active paths from one input to an output on which different MZIs are located and thus, their contributions are reflected in the linear transformation matrix of the application during the programming process. For instance, let us consider a case of programming the SU(4) using an arbitrary linear transformation matrix given by

$$[T_{SU(4)}] = \begin{pmatrix} U_{11} & U_{12} & U_{13} & U_{14} \\ U_{21} & U_{22} & U_{23} & U_{24} \\ U_{31} & U_{32} & U_{33} & U_{34} \\ U_{41} & U_{42} & U_{43} & U_{44} \end{pmatrix}$$

$$= \begin{pmatrix} -0.2341 + 0.0030i & -0.1011 + 0.1765i \\ 0.0953 + 0.2949i & 0.7782 + 0.2674i \\ 0.7987 + 0.2694i & -0.1064yes + 0.2709i \\ 0.2852 + 0.2393i & -0.3399 - 0.2852i \end{pmatrix}$$

$$\begin{pmatrix} 0.5216 + 0.4673i & 0.1664 + 0.6210i \\ 0.1030 + 0.3555i & -0.2120 - 0.2120i \\ -0.1671 - 0.0954i & 0.0357 + 0.4080i \\ 0.1006 + 0.5704i & 0.3290 - 0.4698i \end{pmatrix}. \quad (24)$$

$[T_{SU(4)}]$ is factorized through the process of decomposition to calculate the required phase shifts for the phase shifters of the

TABLE II
CALCULATED PHASE SHIFTS AND THE CORRESPONDING BIAS VOLTAGES OF THE PHASE SHIFTERS FOR PROGRAMMING THE SU(4)

MZI	(1)	(2)	(3)	(4)	(5)	(6)
$\theta\,(Rad)$	1.7453	1.5708	1.3962	1.2217	1.0472	0.8727
$V_\theta\,(V)$	0.38	0.32	0.26	0.35	0.26	0.30
$\phi\,(Rad)$	0.0782	0.1745	0.2618	0.3491	0.4363	0.5236
$V_\phi\,(V)$	0.18	0.31	0.39	0.53	0.62	0.75

MZIs in the device for implementing the matrix by means of the 4×4 reconfigurable optical processor. According to the simulation results shown in Fig. 4(a), each of the obtained phase shifts corresponds to a certain DC bias voltage of the phase shifter. Therefore, to construct the transformation matrix experimentally, the required additional bias voltages are determined and applied to the phase shifters of the characterized MZIs (1) to (6), which are previously set in their C.S. using the measurement results shown in Fig. 10. Table II illustrates the obtained phase shifts from the decomposition of the matrix and their corresponding bias voltages for the phase shifters of the MZI (1) to (6) to add to their $V_{C.S.}$ values to implement the matrix, experimentally.

IV. CONCLUSION

A 4×4 MZI-based optical processor was investigated. The linear transformation matrix of the structure was employed for programming it experimentally. For a given application, a theoretical analysis was developed in detail to extract the required phase shifts from the corresponding linear transformation matrix by decomposing it into that of the MZIs in the SU(4) section of the device. The calculated phase shifts can be used to programme the device through an experimental protocol. The corresponding bias voltages for the calculated phase shifts were determined by using the simulation results of the phase shifter. Our experimental results show that the MZIs in the 4×4 optical processor experience random phase offsets due to fabrication process variations. Consequently, they MZIs are calibrated to mitigate the possible input phase errors, prior to programming the device for an application. The experimental results of the optical processor are in good agreement with those of the 2×2 test structure and the simulation results. Considering the thermal stabilization time of the phase shifters (less than 30 μs) and the total power consumption (approximately 507 mW) of the device for configuration of the MZIs in their appropriate state, such a device with a small footprint would be a promising structure to serve as an accelerator for matrix multiplications in different applications.

ACKNOWLEDGMENT

Authors acknowledge the support from Canadian Microelectronic Corporation (CMC) for the subsidized MPW fabrication through A*STAR Institute of Microelectronics, and the partial financial support from the Canada Research Chairs program.

REFERENCES

[1] D. Perez, E. S. Gomariz, and J. Capmany, "Programmable true-time delay lines using integrated waveguide meshes," *J. Lightw. Technol.*, vol. 36, no. 19, pp. 4591–4601, 2018.
[2] D. A. Miller, "Self-aligning universal beam coupler," *Opt. Express*, vol. 21, no. 5, pp. 6360–6370, 2013.
[3] Y. Shen *et al.*, "Deep learning with coherent nanophotonic circuits," *Nature Photon.*, vol. 11, no. 7, pp. 441–446, 2017.
[4] F. Shokraneh, S. Geoffroy-Gagnon, M. S. Nezami, and O. Liboiron-Ladouceur, "A single layer neural network implemented by a 4×4 MZI-based optical processor," *IEEE Photonics J.*, vol. 11, no. 6, pp. 1–12, Dec. 2019.
[5] N. C. Harris *et al.*, "Quantum transport simulations in a programmable nanophotonic processor," *Nature Photon.*, vol. 11, no. 7, pp. 447–452, 2017.
[6] D. A. Miller, "Self-configuring universal linear optical component," *Photon. Res.*, vol. 1, no. 1, pp. 1–15, 2013.
[7] D. A. Miller, "Establishing optimal wave communication channels automatically," *J. Lightw. Technol.*, vol. 31, no. 24, pp. 3987–3994, 2013.
[8] R. Burgwal *et al.*, "Using an imperfect photonic network to implement random unitaries," *Opt. Express*, vol. 25, no. 23, pp. 28 236–28 245, 2017.
[9] M. Reck, A. Zeilinger, H. J. Bernstein, and P. Bertani, "Experimental realization of any discrete unitary operator," *Phys. Rev. Lett.*, Kobe, Japan, vol. 73, Jul. 1994, pp. 58–61. [Online]. Available: https://link.aps.org/doi/10.1103/PhysRevLett.73.58
[10] F. Le Gall, "Powers of tensors and fast matrix multiplication," in *Proc. 39th Int. Symp. Symbolic Algebr. Comput.*, Waikoloa, HI, USA: ACM, 2014, pp. 296–303.
[11] R. B. Priti, Y. Xiong, and O. Liboiron-Ladouceur, "Efficiency improvement of an O-band SOI-MZI thermo-optic matrix switch," in *Proc. IEEE Photon. Conf.*, Waikoloa, HI, USA, 2016, pp. 823–824.
[12] L. Chrostowski and M. Hochberg, *Silicon Photonics Design: From Devices to Systems*. Cambridge, UK: Cambridge Univ. Press, 2015.
[13] C. K. Madsen and J. H. Zhao, *Optical Filter Design and Analysis*. New York, NY, USA: Wiley, 1999.
[14] G. P. Agrawal, *Lightwave Technology: Components and Devices*. NJ, USA: Wiley, 2004.

Farhad Shokraneh received the B.Sc. degree in electrical engineering from Shahed University, Tehran, Iran, in 2009, and the M.Sc. degree in electrical engineering-communication systems from Lund University, Lund, Sweden, in 2012. He is currently working toward the Ph.D. degree with the Department of Electrical and Computer Engineering, McGill University, Montreal, QC, Canada. His research interests include reconfigurable multiport optical interferometers, optical processors, optical neural networks, photonic integrated circuits, optical–electrical interconnects, and microwave photonics.

Mohammadreza Sanadgol Nezami received the M.Sc. degree in optoelectronics from the Department of Electrical and Computer Engineering, Iran University of Science and Technology, Tehran, Iran, in 2006, and the Ph.D. degree in nanoplasmonics from the Department of Electrical and Computer Engineering, University of Victoria, Victoria, BC, Canada, in 2016. He is currently a Postdoctoral Research Fellow with the Department of Electrical and Computer Engineering, McGill University, Montreal, QC, Canada. His research interests include silicon photonics, optical interconnects, and optoelectronics.

Odile Liboiron-Ladouceur (Senior Member, IEEE) received the B.Eng. degree in electrical engineering from McGill University, Montreal, QC, Canada, in 1999, and the M.S. and Ph.D. degrees in electrical engineering from Columbia University, New York, NY, USA, in 2003 and 2007, respectively. Prior to her graduate studies, she was an Applications Engineer with Teradyne, Boston, MA, USA, from 1999 to 2000, and as a Test Engineer with Texas Instruments, Dallas, TX, USA, from 2000 to 2002. She is currently an Associate Professor with the Department of Electrical and Computer Engineering, McGill University. She has authored or coauthored 55 journal papers and 100 papers in conference proceedings. Her research interests include optical systems, photonic integrated circuits, and photonic interconnects. She holds the Canada Research Chair in Photonics Interconnect. She is a Member of the OSA and SPIE. She was elected on the Board of Governors of the IEEE Photonics Society from 2016 to 2018. She was an Associate Editor of the IEEE Photonics Society from 2009 to 2018, and the IEEE Photonics Society Montreal Chapter Chair since 2010. She has been on several technical program committees at international conferences.